UNIVERSITAT DE BARCELONA

PHYSICS FACULTY

Biophysics Master

Modelling the F_1-ATPase

Biophysics Master project 2007/08:
Rubén Pérez

Supervisor: Jose María Sancho

Contents

Abstract

ATP-synthase is a rotatory molecular machine which synthesizes ATP out of a proton gradient. The F_1 unit is the part of the motor in charge of catalyzing the ATP synthesis out of a rotatory motion induced by the F_0 subunit. F_1 can also work as a motor itself by reversing its working regime hydrolyzing ATP and inducing a rotatory motion (F_1-ATPase). Because of the noisy media in which the F_1-ATPase works, herein we have studied its rotatory dynamics through the Langevin formalism. In order to understand the physical description, the main energy sources acting in the F_1-ATPase have been studied. Including not only the intrinsic energetics of the system but also those sources corresponding to external physical manipulations done in experiments. All these elements are introduced in a simple model in order to understand how the different parts of the motor act together and which is their relevance.

1 Introduction

Science has advanced a lot in the knowledge of the microbiological world, from the first visualization of a cell in the XVII century (just as a paving entity), to the actual one of a complex self-organizing system where millions of chemical processes occur every second. As usual, the more we know, the more unanswered questions arise, and the way the cell works is not an exception. However, the principal ideas of the organization of a cell are understood. In order to have a self-organizing system, a flux of matter and energy and therefore a set of mechanisms is needed in order to maintain this situation out from equilibrium. The set of molecules that carry this energy transduction and therefore that perform the working activities in the cell are called protein molecular machines [1]. The name is very suitable since a behaviour similar to that of handmade macroscopic machines can be observed when taking a closer look to such proteins (that were constructed more than 3000 millions years before). This way, the observables that can be measured and that characterize macroscopic machines such as speed or efficiency (usually very high in molecular machines) are also the observables to be measured in molecular machines.

Molecular machines take many different forms and functions inside the cell. Ranging from the kinesins, whose function is to perform active transport inside the cell across microtubules, to the skeletal muscle myosin, whose role is that of contracting the muscles. In spite of all their differences, all of them need fuel to perform such work. the usual ingredients in this process are the hydrolysis of the ATP molecule or the ion flux across membranes.

keywords: Biophysics, Molecular machines, F1-ATPase, Stochastic dynamics.

1.1 The ATPsynthase

The study of the molecule Adenosine triphosphate (ATP) is probably one of the most frequent topics that have been cause of a Nobel Prize. The first Nobel Prize related with ATP was awarded in 1953. It was the Medicine one and it was presented to Fitz Lipmann for finding that the ATP molecule was the main carrier of energy in the cell. Many processes in living systems take the energy from the ATP hydrolysis, obtaining as residue an ADP (Adeniosine diphosphate) molecule and a phosphate. This way of energy delivering is ubiquitous to every living being from bacteria to eukaryotic animal cells, so the understanding of the aspects involving ATP became an important issue in the biological society.

But, if ATP is used as the bargaining chip in the cell, where and how is ATP formed? The first artificial synthesis of ATP led to the Chemistry Nobel prize in 1957 to the English biochemist Alexander Todd. As years went by, the place where this process takes place in the cell was located. The ATP synthase, a transmembrane protein enzyme found at the membrane of mitochondria was the enzyme responsible for the synthesis of ATP out of its hydrolysis products. In 1978 the chemist Peter Mitchell was awarded also the Chemistry Nobel Prize for its chemiosmotic theory which proposed a mechanism for the ATP synthase for storing energy in ATP molecules through their dehydration synthesis. The chemiosmotic theory claims that the energy stored in ATP is extracted from an ion gradient across the membrane of the mitochondria [2]. So, the role of ATP synthase in the cell is to recharge the ADP molecules by means of the transduction of the energy stored in a ion gradient into ATP through its dehydration synthesis.

The more the technology advanced the more precise was the knowledge of the working of ATP synthase. This way, in 1997, Paul Boyer was awarded the Chemistry Nobel Prize for the observation of a rotatory behavior in the ATP synthase and the statement that it was related with the ATP synthesis [3]. The same Nobel Prize was shared with John Walker, who solved the structure of the hydrophilic part of ATP synthase by means of crystallographic techniques [4]. ATP synthase consists on two important subunits, namely, F_0 and F_1 subunits (Fig.1(a)). On the one hand, the F_0 subunit is the transmembrane subunit in charge of the transduction of the transmembranal ion gradient into a rotation of the γ shaft. On the other hand the globular F_1 subunit is the hydrophilic part of the motor where the catalysis of the ATP production is performed. F_1 is formed by three identical $\alpha\beta$ domains (Fig. 1(b)) so the molecule has a rotational symmetry every third of a turn. F_0 and F_1 communicate through the γ shaft which is the component of the enzyme that breaks the rotation symmetry of the system.

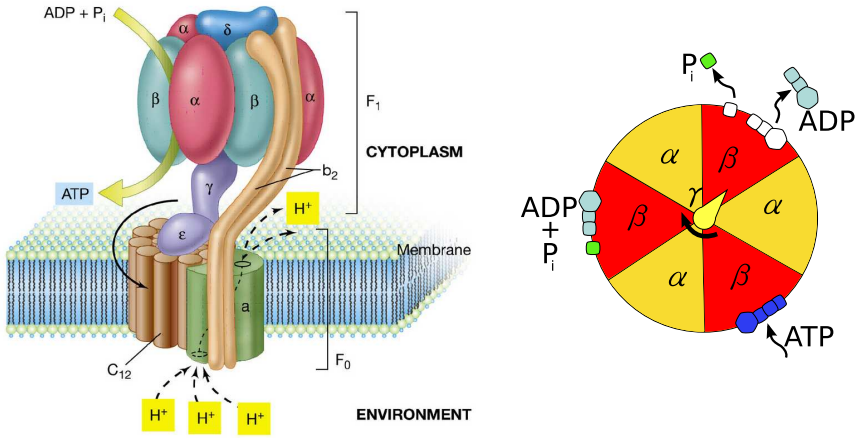

(a) (b)

Figure 1: Different drawings of the F_0F_1ATPsynthase. (a) Complete ATPsynthase. The rotor transmembranal part F_0 rotates driving the motion due to the ion gradient that is coupled to the rotor unit F_1 through the γ shaft. In the F_1 unit the chemical reaction is produced in each one of the β domains. (b) Respresentation of a top view of the F_1-ATPase. The γ shaft turns stepwise with a period of a third of a turn. In each step, each catalytic β site contains an ATP, ADP+Pi or it is ready for the absorption of a new ATP.

The study of the working F_0F_1-ATP synthase, as many other molecules, leads to think of it as a nanometric molecular machine where all its gears do assemble perfectly [3]. The flow of ions through the membrane induces a rotation of the F_0 subunit that in turn produces a rotation of the γ shaft. The rotation of the γ shaft induces a conformational change of the F_1 subunit passing on the energy needed for the ATP dehydration synthesis that is performed in the catalytic β domain (Fig. 1(b)). Carrying on the same analogy with macroscopic machines, the mechanical assemble between F_0 and F_1 resemble to the rotor and stator parts of a motor respectively and are usually referred this way in the literature [5].

Even more interesting is the fact that the working of the motor may be reversed. Taking advantage of the hydrolysis of ATP, the F_1 subunit may rotate the γ shaft that induces the reverse working of F_0 pumping ions across the membrane. Because of this working regime of the F_1 subunit, it is sometimes referred to as F_1-ATPase. All these mechanico-chemical reactions are well synchronized so at each time one of the β domains contains ATP ready to be hydrolyzed, another contains the products of the hydrolysis and the third one is empty in order to receive a new ATP molecule. So, the rotation of the γ shaft is discrete in steps of $2\pi/3$ [6] (Fig. 2(b)). An energetic analysis of each step concludes that the energy needed in order to perform each step is equal to that of the hydrolysis of an ATP. Therefore, in spite of

the noisy media in which the system works (causing seldom backsteps), the efficiency of such a machine is claimed to be nearly 100% [6], entailing the incredible rapport of the components of the ATP synthase.

Although the global behavior of the ATP synthase is already studied, the different physico-chemical mechanisms that are involved in the transduction of chemical energy from the hydrolysis of ATP into rotational movement are still not clear. Different experiments have been performed in order to study which forces are involved in the working of the motor [6] and different models following them [5]. The common element of these experiments is to attach a load to the γ shaft and study how the motor works under such a dissipative force (Fig. 2(a)). For such experiments it is found that for low frictional loads the velocity of the load does not change, and that for high friction loads there is a loglog dependence. With the current technology it is also possible to perform a conservative torque [7] on the load, obtaining information of different nature to that of the dissipative one. Other experiments can be designed in order to measure different mechanical properties of the ATPase, one of them is studying the response of ATPase to different concentration of ATP (Fig. 9(d)). Results show that the more ATP the faster the motor moves, finding a saturation velocity for high concentrations.

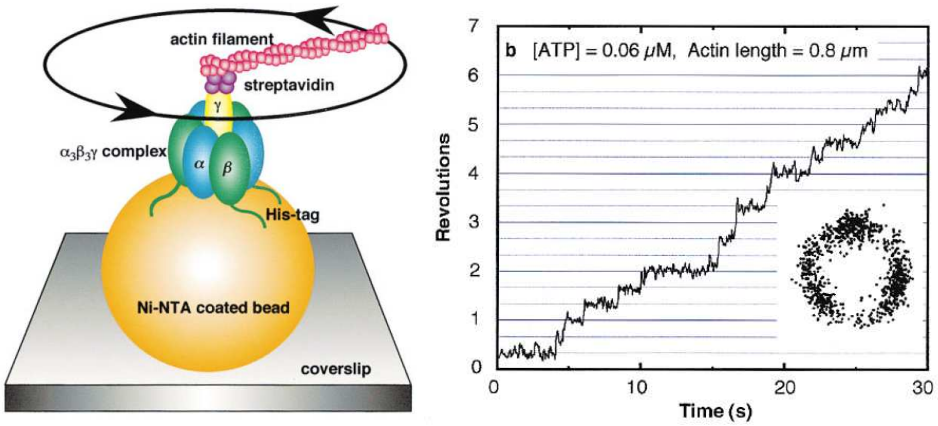

(a) (b)

Figure 2: (a)Experimental system in order to measure the energetics of the F_1ATPase (Not to scale) (b) Experimental results for the F_1ATPase for the trajectory of the filament attached to the γ shaft. It is observed a step-wise rotation of steps equal to a third of a turn. (inset) Trace of the centroid of the load for the experiment. Figures are extracted from [6].

2 The analytical framework: generalities

The biological molecular world has the peculiarity of being located in a length scale where energies of different nature converge [8]. Therefore, when studying a molecular machine every source of force in the system must be chosen carefully. In particular the nanometric scale is the only one in which the thermal effects become comparable to the rest of energy sources. Because of that, statistical mechanics becomes an essential tool to understand the complex physical phenomena that take place in the cell.

2.1 Langevin equation

Once the thermal fluctuations become important in a system, the solution for its trajectories is not deterministic anymore and does change in different realizations. The mechanical motion of such a system can still be described through stochastic differential equations, where an additional term is inserted in Newton movement equations to take care of the thermal fluctuations in the system [9],

$$m\ddot{x} = -\gamma\dot{x} + F_m(x,t) - F_{ext} + \xi(t), \tag{1}$$

where m corresponds to the mass of the object defining the inertial term of the Newton equation. γ stands for the friction coefficient that controls the magnitude of the Stokes friction force that is proportional to the velocity $\dot{x}$. F_m is the motrice force responsible for the natural work of the motor while F_{ext} is the conservative force related to the useful work produced by the motor. Finally $\xi(t)$ is the fluctuation term, which is presented as a white noise defined through

$$\langle \xi(t) \rangle = 0, \tag{2}$$

$$\langle \xi(t)\xi(t') \rangle = 2\gamma k_B T. \tag{3}$$

Note that the intensity of the thermal noise and the friction force depend on the same variable γ. This is not strange since both forces come from the same physical phenomenon and are related through the fluctuation-dissipation theorem.

One of the main characteristics of the dynamics of biological nanometric systems is that the typical length scale is short compared with the typical velocity scale for the friction of the media i.e. the inertial therm of the dynamics decays so rapidly that its dynamics may be neglected when compared with the ones derived from the dissipative forces. This way, equation (1) can be rewritten as,

$$\gamma\dot{x} = F_m(x,t) - F_{ext} + \xi(t), \tag{4}$$

which is known as Langevin equation and is the starting point of any model studying the dynamics of nanometric systems.

2.2 The rotational world

Since the aim of this work is to study a rotatory device, the dynamics of the system does not come epitomized through linear magnitudes but rather by rotatory ones. Therefore, instead of talking of distance and forces, the system must be unraveled through the usage of angular distances ($\theta = x/R$) and torques ($\tau = RF$). These magnitudes are related with their lineal equivalents through the radius of gyration R of the system studied. In this formalism, equation (4) reads,

$$R^2\gamma\dot{\theta} = \tau_m - \tau_{ext} + R\xi(t). \tag{5}$$

Defining the rotational friction coefficient as $\gamma_R \equiv R^2\gamma$ a Langevin equation is obtained equivalent to the initial one but in angular coordinates which also suggests a definition of rotatory thermal noise,

$$R\xi(t) \equiv \xi_R(t) \rightarrow \langle \xi_R(t)\xi_R(t')\rangle = 2\gamma_R k_B T\delta(t-t'). \tag{6}$$

From now on, the R subindex will be dropped out for the sake of simplicity, so the starting equation for any study of the dynamics of a rotatory molecular machine will be,

$$\gamma\dot{\theta} = \tau_m(\theta,t) - \tau_{ext} + \xi(t). \tag{7}$$

The complexity of the model is introduced through the expression of the internal motrice force, which in general has a complex dependence in time and space.

3 Modelling

With a few pondered ingredients it can be derived a model with similar properties to those of a real ATP synthase. This is why models are so important: with the testing of different hypothesis and studying the response of the system, it can be elucidated some of the basic mechanisms that rule the system at the same time that new questions arise obtaining thus a feedback to experimental data.

In order to construct a model of a molecular motor three main aspects of the motor have to be taken into account. First, the kinematic results for which it is observed the *step-wise motion* of the motor. Second, the *mechanico-chemical coupling* where we take into account the energy spent during the working of the motor. Finally, the complete *dynamics of the system*, where we take into account which forces act on the system and how they are introduced in its working.

3.1 Step-wise motion and internal interactions

The first term that is needed in the energetic description of the motor is the internal energy landscape for the *relaxed* state of the system. As it is seen in experimental data (Fig. 2(b)), for the rest state when the system is waiting for an ATP molecule, the γ shaft remains still, oscillating around one of the three equilibrium points that are identified with the β domains of the F_1 globular part.

The only experimental data from such a state are the three symmetric energy minima and the fluctuations around each one of them. Since the fluctuations are symmetric with respect to the minima an angular periodic potential is needed for the rest state. The energetic barrier between the minima must be greater than that of the thermal energy but lower than the energy of the ATP hydrolysis. Since it can be observed backsteps and the coupling ratio of the motor is nearly one, it is expected that the energy for the barrier is closer to the thermal energy than to the ATP hydrolysis one.

The simplest model with such a behavior is the piece-wise linear symmetric ratchet potential, that for the first period reads,

$$V_R(\theta) = \begin{cases} \frac{-3}{\pi} V_0 \theta + V_0 \,; & 0 < \theta < \pi/3 \qquad \text{zone } (I) \\ \\ \frac{3}{\pi} V_0 \theta \,; & \pi/3 < \theta < 2\pi/3 \qquad \text{zone } (II) \end{cases} , \tag{8}$$

being V_0 the energetic barrier to overcome between minima. (I) and (II) stand for the two zones of different slope of the ratchet potential that are repeated periodically (Fig. 3(a)). In spite of the simplicity of such a potential,

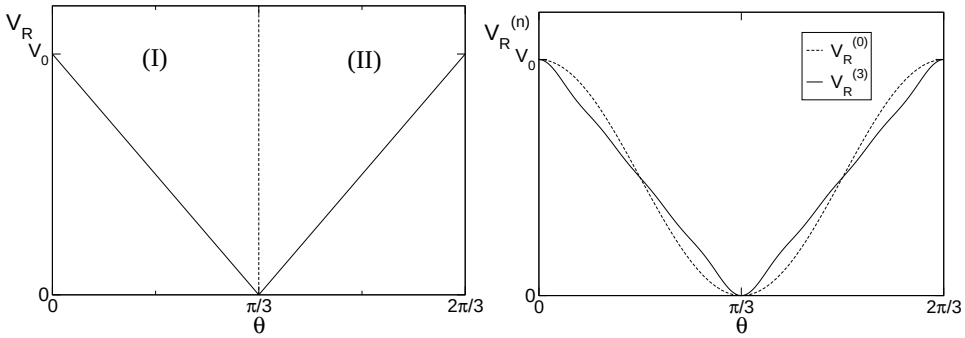

Figure 3: Energetic landscapes for the rest state. (a) The piece-wise linear ratchet landscape is the easiest periodic potential with the expected behavior, (b) The piece-wise linear ratchet can be approximated by a continuous potential.

the ratchet landscape is not analytical in some points so more sophisticated potentials may be introduced. One possible solution is a rescalement of the truncated addition of the Fourier expansion for the ratchet landscape (Fig. 3(b)),

$$V_R^{(n)} = V_0 \frac{Y^{(n)}(\theta) - Y^{(n)}(0)}{Y^{(n)}(\pi/3) - Y^{(n)}(0)}, \tag{9}$$

being,

$$Y^{(n)}(\theta) \equiv \frac{\pi}{2} - \frac{4}{\pi} \sum_{i=0}^{n} \frac{\cos\left((2i+1)(3\theta+\pi)\right)}{(2i+1)^2}, \tag{10}$$

recovering the ratchet potential for the full sum, i.e. $V_R = V_R^{(\infty)}$.

3.2 Mechanico-chemical coupling

From experimental evidences [6] it is known that each step performed during the motion of the system occurs through the absorption of an ATP molecule. The ATP molecule induces a geometrical distorsion of the $\alpha\beta$ structure inducing thus a force on the γ shaft. The result of this process is introduced as a potential for the *excited state* V_E that can be modelled as the linear potential,

$$\langle V_E \rangle = -\frac{3V_1}{2\pi}\theta, \tag{11}$$

being V_1 the torque associated to the ATP absorption (Fig. 4(a)). Chemically this can be understood by means of the *zipper model* [5], which states that the energy of the ATP is not released all of a sudden but little by little through the continuous formation of the different bonds between the ATP

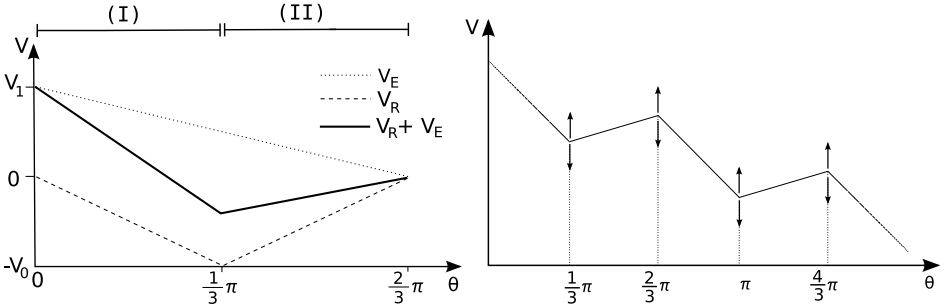

Figure 4: Potential landscape of the model. a) Potential landscape for one of the periods. The total potential is the addition of the symmetric ratchet potential $V_R(\theta)$ and a torque $3/2\pi V_1$. The result is a tilted ratchet potential defining two different slopes for the potential named (I) and (II).b) The resulting mean potential for different periods. Arrows indicate fluctuations.

and the binding site.

The nature of the release of ATP is not fully understood. For the sake of simplicity, the transition between the rest and the excited states can be modelled independently of the internal processes of F_1. As a first approximation, it can be introduced in the model as a fluctuation in the ATP hydrolysis force,

$$V_E(\theta, t) = -\frac{3V_1}{2\pi}\theta \cdot (1 + \eta(t)), \tag{12}$$

being $\eta(t)$ a white noise defined as,

$$\langle \eta(t) \rangle = 0, \tag{13}$$

$$\langle \eta(t)\eta(t') \rangle = 2\sigma\delta(t - t'). \tag{14}$$

Here σ stands for the intensity of the fluctuations. Such a framework introduces a regime transition, so in some instants the overcoming barrier will be high as in the relaxed state and for some other instants the energetic barrier will be low as in the excited one. In fact it can be seen as an ATP saturated system in which there is a continuous income and release of ATP.

The addition of both energetic landscapes, namely, the ratchet and the excitation force, produces a tilted ratchet framework ubiquitous in many molecular motor modelations [10] (Fig.4(b)). The main problem for such an approach is that the physico-chemical coupling is not straightforward so the energy given to the system is not discretized in that of ATP molecules but it is given as a continuous force that combines the effects of the strength of the ATP hydrolysis force through V_1 and the intensity of its fluctuations σ.

3.3 System dynamics and external forces

As usual in molecular studies, the aim molecules of study are too small to be controlled directly or even to be observed. An usual procedure to overcome this difficulty is to attaching a bigger load to the molecule studied and observe how the forces applied on the load affect the working of the main molecule. For the current case, the load is attached to the γ shaft so the load rotates with it (Fig. 2).

The main torque that acts on the load is the *dissipative torque*. This torque comes from the friction of the load so it always opposes to the movement of the system. The dissipative torque will increase with the size of the load and the velocity of the motor. Since the size of the load can be easily controlled, the relation between the frictional torque with the angular velocity of the system is a done fact [6].

An additional torque that can be exerted on the load is a *conservative torque*. This is a constant external torque exerted on the load. A conservative torque is not so easy to perform experimentally as a constant lineal force. Altogether it can be performed by systems such as a the F_0 motor that transducts the chemical energy in a constant torque. Furthermore, some assays have been performed inducing an angular torque in F_1 by using magnetic tweezers [7].

The missing ingredient in order to include such forces in the main equations that describe the system is the coupling between the dynamics of the load and the dynamics of the γ shaft. Since it is expected the coupling to be strong and no great differences appear in the trajectories of both systems, it can be expressed through an elastic coupling. Therefore the joint between both systems is equivalent to that of a torsion spring. The system is thus modeled by the set of equations,

$$\gamma\dot{\theta} = \tau_m(\theta, t) - \kappa(\theta - \phi) + \xi(t), \tag{15}$$

$$\gamma_L\dot{\phi} = \tau_{ext} + \kappa(\theta - \phi) + \xi_L(t), \tag{16}$$

being ϕ the angular coordinate of the load, γ_L the friction rotational coefficient of the load and κ the stiffness of the join between both systems (Fig. 5). The thermal noise acting on the load is defined equivalently as in (6) as,

$$\langle \xi_L(t)\xi_L(t')\rangle = 2\gamma_L k_B T\delta(t - t'). \tag{17}$$

So, the system is finally modeled as two stochastic differential equations that are coupled through a harmonic spring. On the one hand, the equation corresponding to the γ shaft includes all the internal or motrice forces acting on the system $\tau_m(\theta, t)$. On the other hand, the equation corresponding to

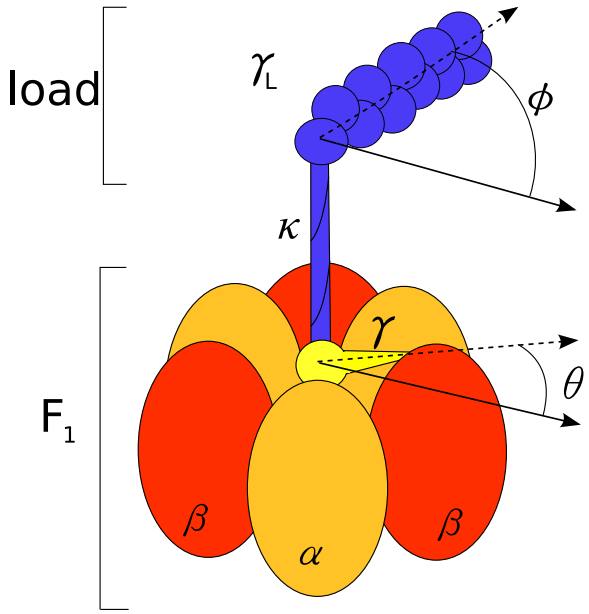

Figure 5: Modelling of the experimental set up for studying the behavior of the F_1 motor. The model consists of two separated systems, the F_1 and the load, joined by an elastic coupling.

the external load that is the observable of the system, includes all the terms corresponding to the external forces: the conservative torque τ_{ext} and the dissipative torque $\gamma_L\dot{\phi}$

3.4 The adiabatic approximation

Dynamic equations describing the system as a function of θ and ϕ (16) may be rewritten in terms of the trajectory of the load, which is the experimentally observable quantity, and the difference in trajectory between the load and the γ shaft,

$$\dot{\phi} = \frac{\tau_{ext}}{\gamma_L} + \frac{\kappa\delta}{\gamma_L} + \frac{\xi_L(t)}{\gamma_L}, \tag{18}$$

$$\dot{\delta} = \frac{\tau_m}{\gamma} + \frac{\tau_{ext}}{\gamma_L} - \left(\frac{1}{\gamma} + \frac{1}{\gamma_L}\right)\kappa\delta + \frac{\xi}{\gamma} + \frac{\xi_L}{\gamma_L}, \tag{19}$$

being δ the relative coordinate that measures the angular distance between both systems $\delta \equiv (\theta - \phi)$. Due to the difficulties of studying analytically a set of coupled differential equations some approximations must be performed. One of them is to the adiabatic limit, which corresponds to the one where the dynamics of the relative coordinate is supposed to be faster than the rest

of the system and, therefore, the variation of δ with time can be neglected,

$$\dot{\delta} \simeq 0 \tag{20}$$

Note that this limit is equivalent to consider a stiff joint κ in which the system shaft-load behaves as a rigid solid. In the adiabatic approximation the difference in position can be computed directly from eq. (19),

$$\delta = \frac{1}{\kappa}\left(\frac{1}{\gamma}+\frac{1}{\gamma_0}\right)\left(\frac{\tau_{ext}}{\gamma_L}-\frac{\tau_m}{\gamma}+\frac{\xi_L}{\gamma_L}-\frac{\xi}{\gamma}\right) \tag{21}$$

So an expression for the trajectory of the load can be found through (18) and (21) following,

$$(\gamma+\gamma_L)\dot{\phi} = (\tau_m+\tau_{ext})+\xi+\xi_L \tag{22}$$

This result states that in the *strong adiabatic limit* the system indeed behaves as a unique solid with a rotational friction coefficient equal to the adding of the two initial ones. This statement refers also to the resultant noise since both noise sources are statistically independent,

$$\langle \xi(t)+\xi_L(t)\rangle = \langle\xi(t)\rangle+\langle\xi_L(t)\rangle = 0 \tag{23}$$

$$\begin{aligned}\big\langle\big(\xi(t)+\xi_L(t)\big)\big(\xi(t')+\xi_L(t')\big)\big\rangle &= \langle\xi(t)\xi(t')\rangle+\langle\xi_L(t)\xi_L(t')\rangle+2\langle\xi(t)\rangle\langle\xi_L(t')\rangle \\ &= 2(\gamma+\gamma_L)k_BT\delta(t-t')\end{aligned} \tag{24}$$

Even though this limit is reasonable, the non-lineal contributions omitted in the analysis have to be taken into account. The origin of such contributions comes from the dependence of τ_m on the γ shaft angular coordinate θ, i.e. the δ has not been completely eliminated from the equations. Nevertheless, since the relative coordinate is small, it can be approximated through a Taylor expansion as,

$$\tau_m(\theta) = \tau_m(\delta+\phi) = \tau_m(\phi)+\delta\tau_m'(\phi)+\mathcal{O}(\delta^2). \tag{25}$$

And therefore, through the adiabatic approximation (20) a new expression for the relative coordinate can be obtained,

$$\delta = \frac{\frac{\tau_m}{\gamma}-\frac{\tau_{ext}}{\gamma_L}+\frac{\xi}{\gamma}-\frac{\xi_L}{\gamma_L}}{\kappa\left(\frac{\varepsilon}{\gamma}+\frac{1}{\gamma_L}\right)}, \tag{26}$$

where the nonlinear terms appear through the variable ε defined as,

$$\varepsilon \equiv 1-\frac{\tau_m'}{\kappa}. \tag{27}$$

Equivalently, the new expression for the trajectory of the load is,

$$\dot{\phi} = \frac{\varepsilon\tau_{ext} + \tau_m + \varepsilon\xi_L + \xi}{\varepsilon\gamma_L + \gamma}. \tag{28}$$

Through this analysis, it can be seen that the coupling of both systems is translated into a modification in a factor ε on the variables corresponding to the dynamics of the load. Note that in general ε its not constant with the position but depends on θ through the variation of the motive torque τ'_m. Therefore, the resultant noise for the *soft adiabatic approximation* is not additive anymore but it has a multiplicative component. For the limit $\kappa \to \infty$ ($\varepsilon \to 1$) the strong adiabatic approximation limit (22) in which both units rotate as a unique particle is recovered.

4 Results

4.1 Analytical results for the adiabatic approximation

Introducing the strong adiabatic approximation to the different assumptions for the working of the model and the applied external forces, the problem is reduced to a Langevin equation reading,

$$\gamma_{eff}\dot{\theta} = -V_R'(\theta) - V_E'(t) - \tau_{ext} + \xi_{eff}(t), \tag{29}$$

Where $\gamma_{eff} \equiv \gamma + \gamma_L$ is the effective friction coefficient predicted by the strong adiabatic approximation. It is worth to note that in such a representation the time and space dependence has been split in both torque terms. While the ratchet potential is constant in time but varies in space, the hydrolyzing torque fluctuates in time.

This description of the system results in a stepwise motion due to the local minima of the potential as in the real F1-ATPase (Fig. 6). Here, the transition between two minima is related with the transition across the energetic barriers.

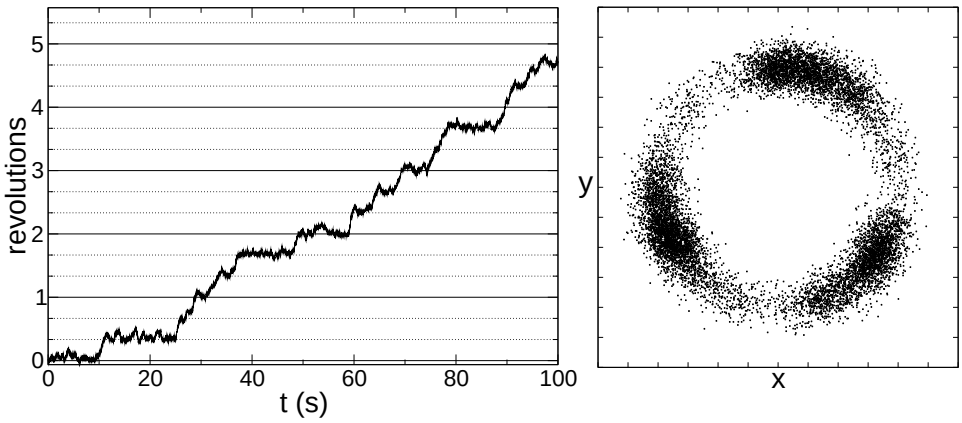

(a) (b)

Figure 6: Simulation of one trajectory of the model. a) Evolution of the angle of the shaft in time. It can be observed that the qualitative behavior corresponds to that of a stepwise movement of the γ shaft of the F1 ATPase. b) Trace of the centroid of the load in arbitrary spatial coordinates. It can be seen that there are three angular equilibrium positions in the system with a occupation density similar to that of experimental data. Parameters used are $\gamma_{eff} = 25\,pN\,nm$, $V_0 = 20\,pN\,nm$, $V_1 = 30\,pN\,nm$ and $\sigma = 0.1\,s^{-1}$.

From the Langevin description it can be written the corresponding Fokker-Planck equation for the probability P for the particle to be in a position θ [9], thus obtaining two partial differential equations, one for each domain (I) and (II) (Fig. 4(a)),

$$\frac{\partial P_I}{\partial t} = A_I \frac{\partial P_I}{\partial \theta} + \alpha \frac{\partial^2 P_I}{\partial \theta^2} \tag{30}$$

$$\frac{\partial P_{II}}{\partial t} = A_{II} \frac{\partial P_{II}}{\partial \theta} + \alpha \frac{\partial^2 P_{II}}{\partial \theta^2} \tag{31}$$

with,

$$A_I \equiv \frac{3}{2\pi} \frac{V_1 + 2V_0}{\gamma_{eff}} - \frac{\tau_{ext}}{\gamma_{eff}}, \quad A_{II} \equiv \frac{3}{2\pi} \frac{V_1 - 2V_0}{\gamma_{eff}} - \frac{\tau_{ext}}{\gamma_{eff}} \tag{32}$$

and,

$$\alpha \equiv \frac{k_B T}{\gamma_{eff}} + \frac{9}{4\pi^2} \frac{\sigma V_1^2}{\gamma_{eff}^2} \tag{33}$$

This way the external conservative torque is introduced in the equation as an addition to the hydrolysis torque but only acting on the drift term of the FP equation. On the other hand the role of the fluctuation in the ATP force only appears in the diffusion term of the FP equation as an increasing term through α, i.e. the fluctuation in the ATP force is equivalent to an increase of temperature of the system.

For the steady state, (30) and (31) become two first order homogeneous differential equations whose general solution is,

$$P_i(\theta) = \frac{J}{A_i} + C_i e^{\frac{A_i}{\alpha}\theta} \qquad i = (I \text{ and } II) \tag{34}$$

Being J the unique flux and C_I and C_{II} two integration constants. Therefore, there must be three boundary conditions in order to find a closed solution.

Due to the symmetry of the system, it can be studied as a finite system with periodic boundary conditions of length equal to a third of a turn, i.e. the exit of a particle from one of the potential hills involves the entering of it into the next one. This way the angular velocity of the particle is related with the flux as $\omega = \frac{2\pi}{3} J$ [10].

Two of the boundary conditions needed are those related to the continuity of the probability in the space. These conditions are imposed at the joint between different regions,

$$P_I(0) = P_{II}(2\pi/3) \tag{35}$$

$$P_I(\pi/3) = P_{II}(\pi/3) \tag{36}$$

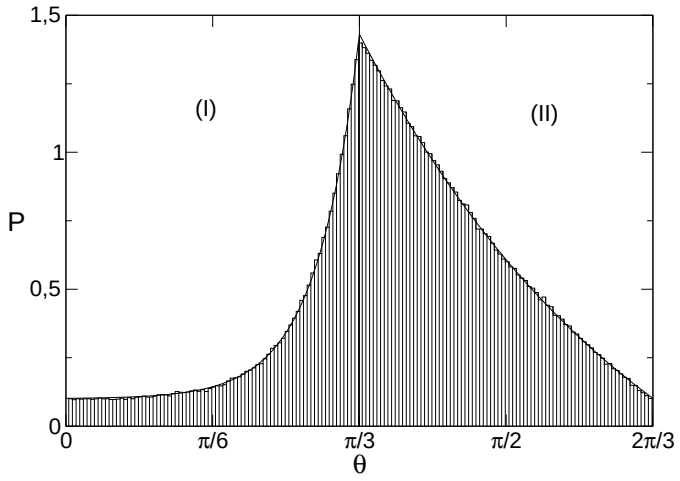

Figure 7: Probability of finding the particle in function of the angle inside one of the periods for the analytical solution (solid line) and a computer simulation (histogram). The probability is the joining of two exponentials giving a maximum at the minimum of the ratchet potential. $V_0 = 20\,pN\,nm$, $V_1 = 30\,pN\,nm$, $\gamma = 20\,pN\,nm\,s$, $\sigma = 0.1\,s^{-1}$

The last condition is the normalization of the probability over both domains,

$$\int_0^{\pi/3} P_I d\theta + \int_{\pi/3}^{2\pi/3} P_{II} d\theta = 1 \tag{37}$$

Obtaining,

$$P_I = J\left(\frac{1}{A_I} + \left(\frac{1}{A_{II}} - \frac{1}{A_I}\right)\frac{1 - e^{-A_{II}\frac{\pi}{3\alpha}}}{1 - e^{-(A_I + A_{II})\frac{\pi}{3\alpha}}} e^{\frac{A_I}{\alpha}\left(\theta - \frac{\pi}{3}\right)}\right) \tag{38}$$

$$P_{II} = J\left(\frac{1}{A_{II}} + \left(\frac{1}{A_I} - \frac{1}{A_{II}}\right)\frac{1 - e^{A_I\frac{\pi}{3\alpha}}}{1 - e^{(A_I + A_{II})\frac{\pi}{3\alpha}}} e^{\frac{A_{II}}{\alpha}\left(\theta - \frac{\pi}{3}\right)}\right) \tag{39}$$

And a expression for the flux,

$$J = \frac{3}{2\pi}\omega = \left(\frac{\pi}{3}\left(\frac{1}{A_I} + \frac{1}{A_{II}}\right) - \alpha\left(\frac{1}{A_{II}} - \frac{1}{A_I}\right)^2\left(\frac{1}{1 - e^{-\frac{A_{II}}{\alpha}\frac{\pi}{3}}} - \frac{1}{1 - e^{\frac{A_I}{\alpha}\frac{\pi}{3}}}\right)^{-1}\right)^{-1} \tag{40}$$

Which gives an analytical expression for the angular velocity of the γ shaft.

The same result for the velocity can be achieved by the averaging over the Langevin equation,

$$\gamma_{eff}\langle\omega\rangle = -\langle V_R'(\theta)\rangle - \langle V_E'(t)\rangle \tag{41}$$

$$= \frac{3}{\pi}V_0\left(\int_0^{\pi/3} P_I d\theta - \int_{\pi/3}^{2\pi/3} P_{II} d\theta\right) + \frac{3}{2\pi}V_1 \tag{42}$$

So, due to the fact that the system spends different time in domains I and II, the averaging of the ratchet potential does not become null and introduces an additional term depending on the probability of occupancy of each zone. Because of the tilting of the potential (Fig. 4) the shaft will spent more time in the zone corresponding to the lower slope (Fig. 7), which is the zone II. Since zone II corresponds to the zone of the ratchet opposing to the advance of the shaft, the average value of the torque exerted by the ratchet landscape opposes the working of the F_1. Therefore, the movement of the γ shaft will be always lower to that of a free brownian particle under a constant torque $\frac{3}{2\pi}V_1$.

While studying the working of the motor in function of the parameter controlling the intensity of the exciting force V_1 (Fig. 8(a)) it can be seen that as expected, the average velocity of the model is lower than that of the brownian particle under a constant torque without the Ratchet potential. Furthermore, this limit is achieved as expected from equation (40) when imposing $V_1 \gg V_0$, i.e. $A_I \simeq A_{II}$

On the other hand, as stated before, the conservative external torque is introduced in the equations by adding it to the hydrolysis torque in the drift term. This way an external torque opposing to the hydrolysis one can stall the system (Fig. 8(b)). The introduction of the external torque is equivalent to a change in the tilting of the Ratchet. As a matter of fact, a value for the conservative torque high enough can induce a backwards rotation.

4.2 Comparison with the experiments

When studying the variation of the velocity with the parameter σ, it is obtained that the increase of the fluctuation through σ always involves an increase of the speed of the system approaching to a saturation velocity value (Fig. 9(b)), just the same behavior was observed for the experimental results with the ATP concentration (Fig. 9(d)). As seen previously, in this model, the ratchet potential always slows down the average velocity of the motor. In the large fluctuation limit, the fluctuations erase the order that involves

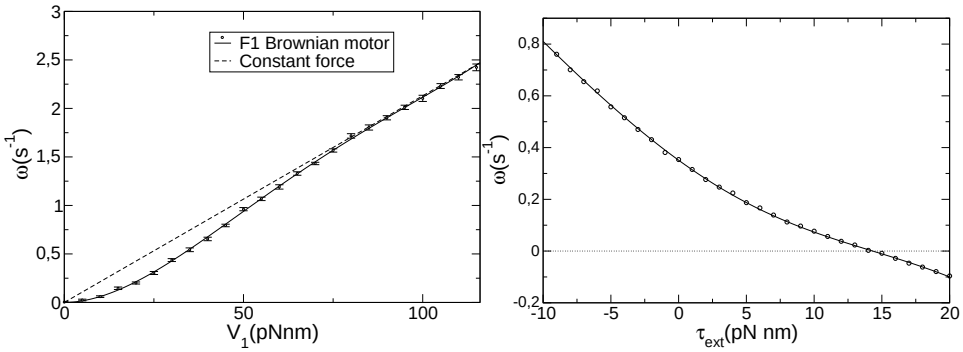

(a) (b)

Figure 8: Relation of the velocity of the system with the main value for the ATP force (a) and the intensity of its fluctuation (b). The full line corresponds to the analytical expression (40) while the points correspond to computer simulation of the strong adiabatic limit Langevin equation (29). The dashed line corresponds to the case in which the particle behaves as a brownian particle moving under a constant external force $3V_1/2\pi$ without any ratchet landscape. This corresponds to the limit for high values of V_1 or σ. Parameters used are $\gamma = 22.5\,pN\,nms$, $V_0 = 20\,pN\,nm$, $V_1 = 30\,pN\,nm$ and $\sigma = 0.1\,s^{-1}$.

the ratchet potential, so the system behaves as a particle acting under a constant force. This limit is analogue to the saturation velocity found in real F_1 ATPase, where for a high concentration of ATP dwell times disappear. This is what happens in the brownian F_1 where the disappearing of the ratchet involves the disappearing of the minima of energy and therefore the dwell times. However, as has been previously mentioned, the dwell times do not only depend on sigma but also in the rest of parameters of the model, so even without a fluctuating force ($\sigma = 0$), there is still a net displacement in the system due to the tilting of the ratchet and the thermal fluctuations. This saturation velocity for low values of σ corresponds to the situation in which the thermal noise rules over the fluctuation of the excitation force in the term α, so all the displacement over the energetic barriers is overcome thermaly.

Since the time scale of the system can be redefined through the parameter γ_{eff} in the original equation, the increase in γ_{eff} may be regarded as a slowing down of the system. So, an increase in the friction coefficient will not stall it $\omega \sim (\gamma)^{-1}$. Splitting the term γ_{eff} in two corresponding friction terms, γ and γ_L, allows one to study the effect of the dissipative force in the system (Fig. 9(a)). It can be seen that the qualitative behavior is similar to that of the experimental results (Fig. 9(c)) with two different regimes: One corresponding to the low friction limit where the velocity of the system remains constant, and the other for high friction loads in which is found a

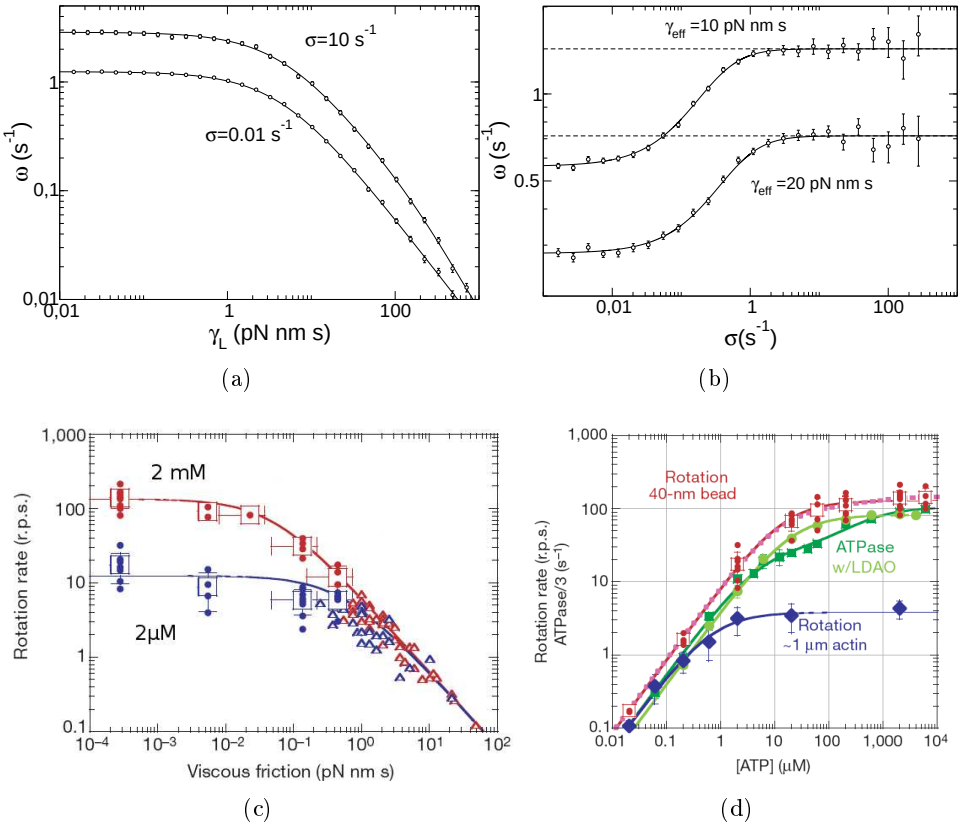

Figure 9: Comparison of the model (top) with experiments (bottom). (a) Relation between the rotational friction coefficient of the load and the velocity of the motor. The friction coefficient slows down the motor without stalling it. (b) Relation between the velocity and the fluctuations on the external force. Flucutations increase the speed of the motor. (c) Relation between the friction coefficient of the load and the velocity of the system for different ATP concentrations. Full lines correspond to a fit for the theoretical approximation for the system as a brownian particle under a constant force. (d) Relation between the velocity of the load and the ATP concentration. Experimental figures are extracted from [11]. Parameters used, $\gamma = 20\,pN\,nm\,s$, $V_0 = 20\,pN\,nm$ and $E_1 = 30pN\,nm$.

loglog depence. Both limits can be deducted for the behavior of a brownian particle under a constant force. However, as has been seen before, since the average $\langle V_R \rangle$ is in general different from zero and dependent on γ_{eff} the relation is more complicated than a simple brownian particle.

4.3 Elastic coupling: numerical results

Since the ratchet intrinsic torque is not derivable at every point it cannot be studied analytically the soft adiabatic approximation (28). However, the complete system without any adiabatic approximation can be studied through numerical analysis.

There are two main differences between the adiabatic and the non-adiabatic system. On the one hand, the information shared by both elements (shaft and load) is damped by the coupling. Oppositely to the adiabatic one in which any force applied at any element was transmitted instantly to the whole system. On the other hand there is a competition of the evolution velocity of both elements so the slower evolution will rule the global behavior of the system oppositely to the adiabatic approximation in which only one dynamic evolution matters. These effects can be observed through the angular probability distribution of both elements (Fig. 10).

For high values of γ and low values of γ_L without any external torque it can be observed that the probability distribution for the shaft is equivalent to that of the adiabatic approximation. The distribution for the load is the same one but diffused in the angle coordinate (Fig. 10(a)). This is so since $\gamma > \gamma_L$ entails that the evolution of the shaft will be slower than the load one and will rule the evolution of the system. Altogether the distribution of the load is not equal to that of the shaft due to its high fluctuations and the damping of the coupling.

On the other hand, for the limit in which the friction of the load is higher than the friction of the shaft ($\gamma_L > \gamma$) a different behavior is observed in which the behavior of both elements is far from the adiabatic one (Fig. 10(d)). In this limit the response of the load is slow compared with the response of the shaft and will rule the evolution dynamics.

In spite of this damping of the order exerted by the torques of the system, the global behavior of the system is similar to that of the adiabatic one. On the one hand, the dissipative torque is not able to stall the system and has the same shape as in experimental results (Fig. 11(a)). On the other hand the external conservative torque is able to stall it and even reverse the motion of the system (Fig .11(b)). These similitudes come from the fact that

although the probability distribution changes, the term corresponding to the average of the ratchet potential $\langle V_R \rangle$ does not change so much. Therefore, for the brownian rathcet F1-ATPase the elastic coupling becomes important when it is wanted to extract properties of the motor from the fluctuation of the measurement.

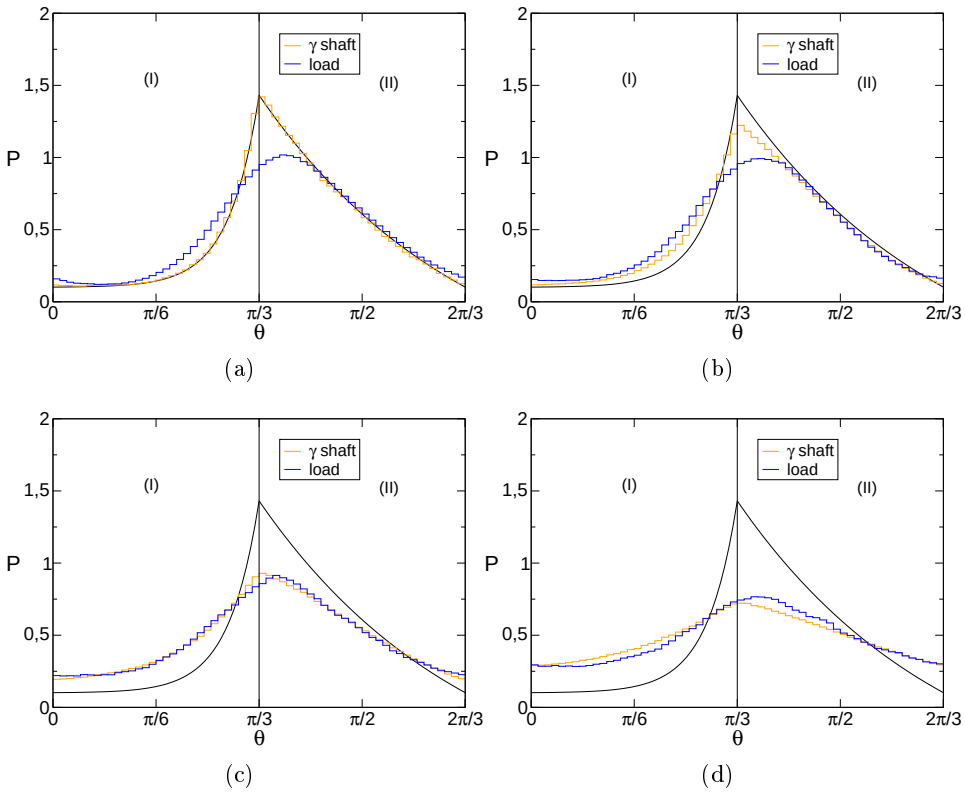

Figure 10: Probability distribution of the load and the γ shaft for the coupled system. Due to the elastic coupling, the system does not behave completely as a rigid solid. In general the distribution of the γ shaft is sharper to that of the load. The solid line corresponds to the analytical results for the rigid solid one with $\gamma_{eff} = 20\, pN\, nm$. a) $\gamma = 19 pN\, nm\, s$, $\gamma_L = 1 pN\, nm\, s$, b) $\gamma = 5 pN\, nm\, s$, $\gamma_L = 15 pN\, nm\, s$, c) $\gamma = 2 pN\, nm\, s$, $\gamma_L = 18 pN\, nm\, s$, d) $\gamma = 1 pN\, nm\, s$, $\gamma_L = 19 pN\, nm\, s$. The rest of the values are $\kappa = 100\, pN\, nm$ and those corresponding to Fig. 7

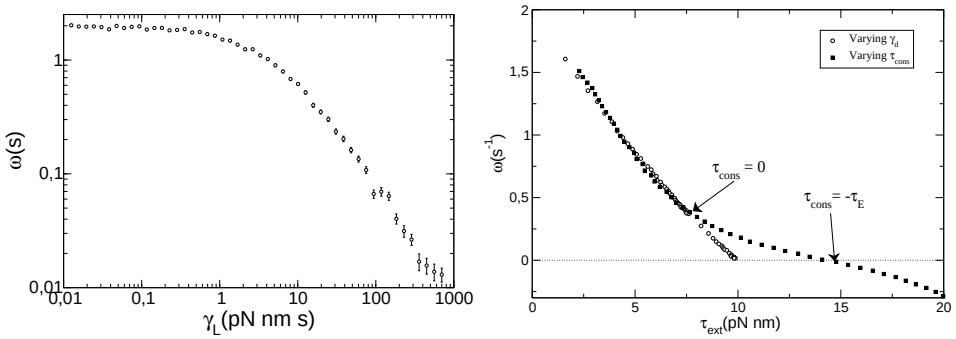

(a) (b)

Figure 11: Results for simulations for the brownian motor. a) The increase of the friction of the load slows down the γ shaft but does never stall it. $\gamma = 5\,pN\,nms$, $V_0 = 20\,pN\,nm$, $V_1 = 30\,pN\,nm$ and $\sigma = 0.1s^{-1}$ b)Relation between the angular velocity of the system and the total external torque τ_{tot}. Through the variation of the conservative torque (black squares) simulations show that a high value of the conservative torque may stall the motor and even reverse its motion. To the left of the point $\tau_{ext} = 0$, the external torque assists the rotation of the system. $\gamma = 5\,pN\,nms$, $\gamma_L = 17.4\,pN\,nms$ $V_0 = 20\,pN\,nm$, $V_1 = 30\,pN\,nm$, $\sigma = 0.1s^{-1}$ $\kappa = 100\,pN\,nm$. On the other hand simulations show the relation between the dissipative torque (white circles) and the velocity of the system for the same values obtained in a).

5 Conclusions

Since molecular motors act as essentially classical objects, in spite of the thermal fluctuations acting of the system it is easy to introduce phenomenological heuristic forces in their modelation. Altogether, due to the stochastic nature of the problem the final analytical solution may not be easily achieved or even it may not exist. On the other hand the complex relation of these fluctuations may have the answer to construct such an efficient system in the molecular scale so it must be studied carefully as one of the main ingredients for the working of a motor.

This effect is already present in the elastic coupling between the γ shaft and the load. The load attaching is an ubiquitous technique to many biomolecular experiments and it has been shown how with a simple elastic coupling, fluctuations at each end of the joint may introduce important terms affecting to the working of the whole system, specially in zones with large force variation such as an energetic barrier.

From the results obtained for the brownian F_1-ATPase motor it has been shown how with the simplest model available it can be indeed predicted a stepwise motion for the F_1-ATPase. Furthermore, with this model the ef-

fects of different external torques can be studied. On one hand, the effect of a conservative torque that may reverse the motion of the γ shaft but this requires a more complicated and not so developed experimental setup. On the other one hand, the acting of a friction force that is always dependent on the velocity of the system and it is not able to stall the system.

With this model it has been also possible to study the effects of the elastic coupling of two systems and how the order created by the forces is damped by the effect of the coupling. Such a study is important because usually the measurable magnitude is the resulting from a coupling so the observed effects are not identical to those of the strong adiabatic coupling.

The main lack of this model for the F_1-ATPase is a correct mechanico-chemical coupling that introduces the energetic consumption of ATP per turn. Neither the study of the relaxation process is taken into account. However, these simplifications have helped in order to study the rest of the effects already mentioned without extra complications.

6 Perspectives

Once the effect of the elastic coupling and the conservative and dissipative torques are well integrated in the model, the next step is to take into account more carefully the mechanico-chemical aspects of the motor. This can be introduced by means of a flashing ratchet formulation. Such a formulation does not only take care of the energy input needed to perform work in the system but also the synchronization of both landscapes, excited and relaxed, in order to improve the velocity of the motor. A first approximation to such a behavior may be achieved by means of a dichotomous noise on the hydrolysis torque (Fig. 12(a)),

$$V_R = \frac{3}{2\pi} V_1 \theta \eta(t), \tag{43}$$

where $\eta(t)$ is the dichotomous noise that switches between two states: 0 and 1, defined through the probability of the two possible jumps, w_{01} and w_{10}.

Such a model takes into account the nature of the excitation landscape. The dwell time of the motor between different steps has been found to be dependent uniquely on the concentration of ATP in the media [6]. Supposing that the absorption process is a Poisson process so the rate of reaction is constant in time, the resulting probability distribution for the dwell times between reactions should follow an exponential distribution. Although experimental results fit well with the Poisson process theory, once the ATP enters the system, the following reactions are not completely deterministic and some other exponential terms may correct the initial one [12][13][14].

As far as the deexcitation process is concerned, some assays show that the power stroke for the consumption of the ATP does not occur all of a sudden but in two substeps of 80^o and 40^o respectively [12][11]. These substeps may be related with two power strokes: on the one hand, the one related with the ATP hydrolyzing, and on the other hand, the energy related to the release of the ADP to the media triggered by the position of the γ shaft. Therefore, the deexcitation process is not so straightforward as the excitation one and may contain important effects for the understanding of the great efficiency of the motor. Approximations to the understanding of these effects may be introduced by more complex conditional flashing ratchet potentials (Fig. 12(b)).

Since one of the aims of modeling is to understand the different role that the different pieces of the system play, is easy to extend the obtained information to similar systems. This way the understanding of the working of the F_1-ATPase motor can also drive to understanding of the direct working regime of the F_1 unit. Also, all the rotational Langevin formalism with the

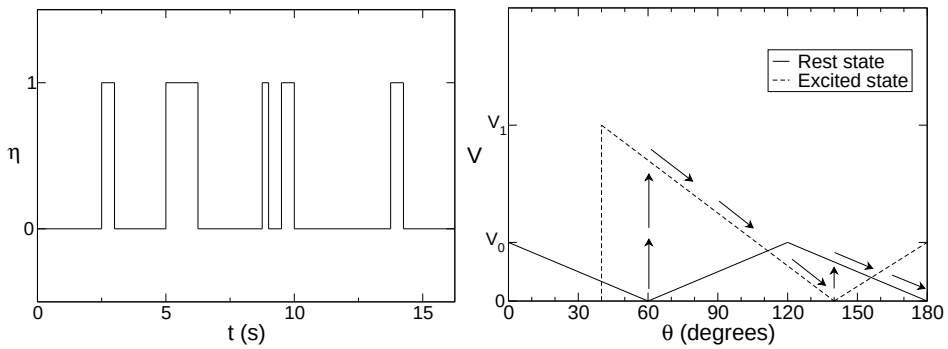

(a) (b)

Figure 12: a) Example of the evolution of a dichotomous noise in time. The hydrolysis potential is activated in exponentially distributed impulses. b) Proposal for a flashing ratchet with the two substep motion.

study of the effect of the applied torques can be used to the understanding of the working of the F_0 unit and therefore the whole ATPsynthase. All this study does not end with the ATP synthase but is useful for other rotational motors such as the Bacterial Flagellar motor.

A Numerical tools

The stochastic simulations have been performed with a simple Euler algorithm that for a Langevin equation reads,

$$x(t+\Delta t) = x(t) + \frac{f(t)}{\gamma}\Delta t + \sqrt{\frac{2k_BT\Delta t}{\gamma}}\eta \tag{44}$$

Being η random gaussian distributed numbers with zero mean and variance equal to one.

A more sophisticated Heun algorythm has not been chosen in order to speed up the simulations. Nevertheless, this is well justified because in a stochastic simulation the stochastic fluctuations become bigger than the corrections gained than by the Heun method. This is why in such a simulation efforts should be taken in performing averages over many runs with a small enough time step, taking into account the quality of the random numbers used for the simulations. The random numbers used in the simulations of the work are generated with the Mersenne Twister random number generator [15].

References

[1] Howard, J. *Mechanics of Motor Proteins and the Cytoskeleton.* Sinauer associates, Inc. (2001).

[2] Mitchell, P. Coupling of phosphorilation to electron and hydrogen transfer by a chemi-osmotic type of mechanism. *Nature* (1961). **191**, 144–148.

[3] Boyer, P. The ATP synthase: a splendid molecular machine. *Annu. Rev. Biochem.* (1997). **66**, 717–749.

[4] Abrahams, J., Leslie, A., Lutter, R. & Walker, J. Structure at 2.8 å of F_1-ATPase from bovine heart mitochondria. *Nature* (1994). **370**, 621–628.

[5] Oster, G. & Wang, H. Reverse engineering a protein: the mechanochemistry of ATP synthase. *Biochimica et Biophysica Acta* (2000). **1458**, 482–510.

[6] Yasuda, R., Noji, H., Kinosita, K.J. & Yoshida, M. F_1-ATPase is a highly efficient molecular motor that rotates with discrete 120^o steps. *Cell* (1998). **93**, 1117–1124.

[7] Hirono-Hara, Y., Ishizuka, K., Kazuhiko Kinosita, J., Yoshida, M. & Noji, H. Activation of pausing F_1 motor by external force. *PNAS* (2005). **102**, 4288–4293.

[8] Philips, R. & Quake, S.R. The biological frontier of physics. *Physics today* (May 2006).

[9] Gardiner, C. *Handbook of Stochastic Methods: for Physics, Chemistry and the Natural Sciences*. Springer (2004).

[10] Reimann, P. Brownian motors: noisy transport far from equilibrium. *Physics Reports* (2001). **361**, 57–265.

[11] Yasuda, R., H., N., Yoshida, M., Kinosita, K.J. & Itoh, H. Resolution of distinct rotational substeps by submillisecond kinetic analysis of F_1-ATPase. *Nature* (2001). **410**, 898–904.

[12] Shimabukuro, K., Yasuda, R. & et al. Catalysis and rotation of F_1 motor: Cleavage of ATP at the catalytic site occurs in 1 ms before 40^o substep rotation. *PNAS* (2003). **100**, 14731–14736.

[13] Higuchi, H., Muto, E., Inoue, Y. & Yamagida, T. Kinetics of force generation by single kinesin molecules activated by laser photolysis of charged ATP. *PNAS* (1997). **94**, 4395–4400.

[14] Hua, W., Young, E., Fleming, M. & Gelles, J. Coupling of kinesin steps to ATP hydrolysis. *Nature* (1997). **388**, 390–393.

[15] Matsumoto, M. & Nishimura, T. *ACM transactions on modeling and computer science* (1998). **8**, 3–30.